

NUMERICAL STUDY OF MIXED CONVECTION HEAT TRANSFER USING OSCILLATING TWO CYLINDERS INSIDE A CAVITY FILLED WITH A HYBRID NANO FLUID CU-AL₂O₃-WATER

Rusul Abbas Alwan^{1,2*}, Nabil Jamil Yasin³, Hameed k. Hamzah⁴

¹Technical Engineering College-Baghdad, Middle Technical University, Baghdad, Iraq,

²Mechanical Power Technical Engineering Department, College of Engineering and Technology, Al-Mustaqbal University, Hilla, 51001, Babylon, Iraq

³Al_Amarah University College, Iraq

⁴College of Engineering, University of Babylon, Iraq

Emails: abc4005@mtu.edu.iq, rusul.abbas@uomus.edu.iq, Nabiljamil58@gmail.com, eng.hameed.hamzah1@uobabylon.edu.iq

Abstract - This study investigates the effect of mixed convection for two solid cylinders in a square cavity subjected to vertical sinusoidal vibration. The cavity is filled with water-based hybrid nanofluid. To perform the numerical simulation of the two-dimensional square cavity, the Galerkin finite element method was used. The outer walls of the cavity were set at a low temperature while the two cylinders were heated to equal temperatures. Cu₂O₃ and Al₂O₃ nanoparticles were used with water to generate the hybrid nanofluid. Several variations of non-dimensional parameters, such as Rayleigh number (10^3 and 10^5), oscillation amplitude (0 and 0.15), and frequency (0.5 and 40), were considered, while a constant Prandtl number (Pr=6.2) and period (2), were considered, and their effects on the intra-cavity flow and heat transfer were studied. The results showed that increasing the oscillation frequency and amplitude enhanced the heat transfer. It also showed that increasing the Rayleigh value from 10^3 to 10^5 significantly enhanced the thermal performance. The Nusselt number increased by approximately 34.4% for cylinder A and 35.5% for cylinder B at A=0.

Keywords: Hybrid nanofluid and Oscillatory cylinder, Nanofluid nanoparticles and mixed convection.

1. Introduction

Natural convection resulting from the oscillation of two circular cylinders within a two-dimensional square cavity has been studied because of its importance in many engineering applications, such as clean energy systems, air conditioning and refrigeration equipment, thermal energy storage systems, nuclear reactors, high-efficiency thermal equipment, micro chemical reactors, medical and biological fields (such as drug delivery).

Researchers have conducted several studies focusing on convective heat transfer and entropy generation within closed and open cavities of various shapes containing various fluids. Some of the previous research in the literature related to the natural convection heat transfer inside non-square cavities to improve natural convection heat transfer

are presented in this section, [1] and [2]. Natural convection heat transfer in a square cavity was investigated. The left vertical wall was subjected to heat flux. The result showed that the heat transfer near the upper wall was the highest rate [3].

Given the importance of increasing heat transfer for the necessary needs in many industrial applications, [4] presented a set of solutions to improve natural convection heat transfer in non-square cavities filled with porous media or hybrid nanofluid.

Some studies indicated that the flow structure and heat exchange are significantly sensitive to different dimensions and shapes of the cavities, both with and without nanofluids [5] and [6]. When using a hybrid nanofluids, heat transfer is enhanced compared to pure water placed in a U-shaped cavity with a hot, wavy wall [7]. The results of the effect of a magnetic

field applied to a nanofluid inside a cavity indicated that the Nusselt number is enhanced with increasing the volume fraction of the nanofluid [8]. To improve the heat exchange process, some researchers have turned to generating vibrations to increase the heat mixing process. [9] indicated that vibrational effects are significantly noticeable at the maximum Reynolds and Darcy values. While at low Reynolds and Darcy values, buoyancy forces are dominant. In their work, [10] found that higher frequencies were the most effective in enhancing heat transfer. However, increasing the magnetic field negatively affected the improvement of heat transfer. Placing a rotating cylinder in the centre of a cavity filled with a nanofluid and a porous medium overlapped with it led to an increase in the flow intensity and enhanced the heat transfer process as reported by [11]. Effect of increasing the length of the heated wall of a quarter-circle cavity filled with a Cu-Al₂O₃/water hybrid nanofluid was investigated in [12]. During the vibration of two elliptical bodies at different frequencies and amplitudes, the lower and upper walls heated up and cooled down, respectively. The vertical walls provide thermal insulation. Increasing the Rayleigh number and the length of the hot wall makes the temperature gradient lines denser near the hot and cooled walls. Heat generation from the hot source increases with increasing hot wall length [13]. Despite the vast number of studies presented by researchers and scientists in the field of mechanical engineering, which focused on studying heat exchange and entropy generation, in addition to research that studied the physical and chemical properties of nanofluid and hybrid nanofluid, the sinusoidal vibration of cylinders placed within a closed cavity filled with a hybrid nanofluid Cu-AL₂O₃/water. remains an insufficiently explored research area, and is considered one of the important modern topics that has not received the attention it deserves. The complex relationship between mechanical vibrations and entropy generation in a closed cavity in the presence of a hybrid nanofluid is a major scientific challenge. Therefore, this study sought to bridge this fundamental research gap by implementing high-precision numerical simulations using COMSEL 6.2, an advanced program that provides a deep physical representation of the combined effects of a hybrid nanofluid within a closed cavity and the sinusoidal vibration effect of two cylinders moving in the same direction, both rising upward and then descending downward, influenced by several variables,

including oscillation amplitude, frequency, and leigh number values.

The study also seeks to uncover the most important precise physical mechanisms that govern the heat exchange process in mixed convection and the flow behaviour within the cavity in the presence of vibrations.

This helps build an advanced scientific foundation that can be used in the design of some advanced thermal systems in future engineering applications.

In this work, heat transfer phenomenon and entropy generation in a hybrid nanofluid inside a square cavity were investigated. Effect of the oscillatory motion of the two cylinders inside the cavity are investigated by changing the amplitude and frequency of the vibratory motion. In addition, a parametric study involves studying effect of several parameters are introduced as well. In addition, a parametric study was introduced to investigate effect of several parameters, such as Rayleigh number, oscillation frequency, oscillation amplitude, and oscillation period on the entropy generation and heat transfer inside the cavity. These ideas have a practical importance for engineering designers in modern technical fields, including their applications in thermal systems and devices such as clean energy systems, heat exchangers, thermal storage units, and small cooling systems used in electronic devices. The topic provides a comprehensive analysis of flow and heat transfer within the cavity using a range of evaluation tools, including thermal gradient lines, entropy generation, velocity trend lines, local Began number, and local and average Nusselt number.

1.1 Cavity Geometry

The geometrical description of the cavity in this work is presented in Fig.1. The two cylinders inside the cavity are subjected to a sinusoidal oscillatory motion and immersed in the nanofluid. The nanofluid consists of aluminium oxide (Al₂O₃) and copper (Cu) nanoparticles in water inside the square cavity. The nanoparticles are assumed to be in dynamic and thermal equilibrium without any agglomeration or sedimentation, i.e., they are suspended and stable. The two oscillating cylinders oscillate along the y-axis, and their specific displacement can be defined by the equation $y = A \sin 2\pi ft$, where f is the oscillation frequency and A is the oscillation amplitude. This process involves redirecting the flow toward or away from the hot source and generating multi-circulation fluid

patterns. This, in turn, increases the heat transfer efficiency by reducing the thickness of the thermal boundary layer near the hot source wall. This increased control of heat transfer can be achieved by the motion of the oscillating solid cylinders.

The thermophysical properties of the nanoparticles used in the study, as well as those of water, are given in Table 1.

Table 1. Thermophysical properties of the components of Cu-Al₂O₃/water [14] and [15]

Physical properties	Water	Al ₂ O ₃	Cu
$c_p / J \text{ kg}^{-1} \text{ K}^{-1}$	4179	765	385
$k / W \text{ m}^{-1} \text{ K}^{-1}$	0.613	40	401
$\rho / \text{kg m}^{-3}$	997.1	3970	8933
β / K^{-1}	21×10^{-5}	0.85×10^{-5}	1.67×10^{-5}
$\alpha / \text{m}^2 \text{ s}^{-1}$	1.47×10^{-7}	131.7×10^{-7}	1.11×10^{-4}
$\mu / \text{kg m}^{-1} \text{ s}^{-1}$	8.9×10^{-4}	-	-

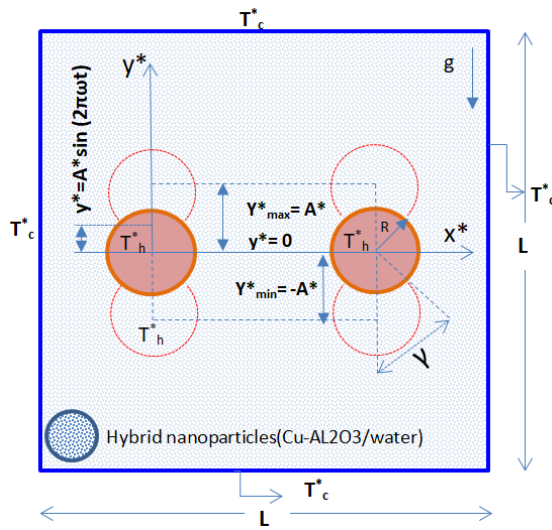


Figure 1: Geometrical Description of the cavity

2. Mathematical Modeling

The Boussinesq approximation is applied to simulate density fluctuations at the buoyancy limit. The heat transfer equation takes into account convection and conduction from the energy equations, ignoring viscous dissipation and radiation effects. With the assumptions made above, the governing equations can be represented as follows [13]:

A. Continuity Equation:

$$\nabla^* \cdot \mathbf{u}^* = 0 \quad (1)$$

B. Momentum Equation:

$$\frac{\delta \mathbf{u}}{\delta t} + (\mathbf{u}^* - \mathbf{w}^*) \nabla^* \cdot \mathbf{u}^* = - \left(\frac{1}{\rho_{\text{hnf}}} \right) \nabla^* \cdot \mathbf{P}^* + \frac{\mu_{\text{hnf}}}{\rho_{\text{hnf}}} \nabla^{*2} \cdot \mathbf{u}^* + \beta_{\text{hnf}} \mathbf{g} (T^* - T_c^*) \quad (2)$$

C. Energy Equation:

$$\frac{\delta T^*}{\delta t} + (\mathbf{u}^* - \mathbf{w}^*) \nabla^* \cdot T^* = \alpha_{\text{hnf}} \nabla^{*2} T^* \quad (3)$$

In the above equations, \mathbf{u}^* is the velocity vector with components u in the x direction and v in the y

direction, while \mathbf{w}^* is the velocity of the moving mesh, p is the fluid pressure, T^* is the fluid temperature, \mathbf{g} is the gravitational acceleration vector.

α_{hnf} is the thermal diffusivity and μ_{hnf} is the dynamic viscosity of the hybrid nanofluid. ρ_{hnf} is the density of the hybrid nanofluid, and β_{hnf} is the volumetric thermal expansion coefficient of the hybrid nanofluid.

The initial and boundary conditions (BC) imposed on the domain are:

BC1: Outer walls of the cavity

$$T = u = v = 0 \quad (4a)$$

BC2: Oscillating cylinders

$$T = T_h^* \quad (4b)$$

$$\mathbf{u}^* = d\mathbf{y}^*/dt = 2 A^* \pi \omega \cos(2\pi\omega) \quad (4c)$$

The non-dimensional analysis is used to determine the following dimensionless parameters:

$$\begin{aligned} \frac{t \alpha_f}{L^2} &= \tau, \quad \frac{x^*}{L} = x, \quad \frac{y^*}{L} = y, \quad \frac{(L^2)}{(\rho_f \alpha_f^2)} \cdot P^* = P \\ \frac{u^* L}{\alpha_f} &= u, \quad \frac{w^* L}{\alpha_f} = w, \quad \frac{v_f}{\alpha_f} = \text{Pr}, \quad \frac{\nabla^*}{1/L} = \nabla \\ \frac{(T^* - T_c^*)}{(T_h^* - T_c^*)} &= T, \quad \frac{(g \beta (T_h^* - T_c^*) L^3)}{(v_f \alpha_f)} = \text{Ra}, \quad \frac{\nabla^{*2}}{1/L^2} = \nabla^2 \end{aligned} \quad (5)$$

Non-dimensional Equations:

Based on the nondimensional parameters presented above, eqns (1, 2, 3) can be written as [13]:

$$\nabla \cdot \mathbf{u} = 0 \quad (6)$$

$$\begin{aligned} \frac{\partial \mathbf{u}}{\partial \tau} + (\mathbf{u} - \mathbf{w}) \cdot \nabla \mathbf{u} = \\ - \left(\frac{\rho_f}{\rho_{\text{hnf}}} \right) \nabla p + \left(\frac{\rho_f}{\rho_{\text{hnf}}} \right) \left(\frac{\mu_{\text{hnf}}}{\mu_f} \right) \text{Pr} \nabla^2 \mathbf{u} + \\ \left[\frac{(\rho \beta)_{\text{hnf}}}{(\rho_{\text{hnf}} \beta_f)} \right] \text{Pr Ra T} \end{aligned} \quad (7)$$

$$\frac{\partial T}{\partial \tau} + (\mathbf{u} - \mathbf{w}) \cdot \nabla T = (\alpha_{\text{hnf}} / \alpha_f) \nabla^2 T \quad (8)$$

In equation (7), Pr is the Prandtl number and Ra is the Rayleigh number, and equation (8) $\alpha_{hnf} = k_{hnf} / (\rho c_p)_{hnf}$, $(\rho C_p)_{hnf}$.

$$(\rho\beta)_{hnf} = (1 - \varphi_{hnp})(\rho\beta)_f + (\varphi.\rho\beta)_{Al2O3} + (\varphi.\rho\beta)_{Cu} \quad (10)$$

$$(\rho C_p)_{hnf} = (1 - \varphi_{hnp})(\rho C_p)_f + (\varphi.\rho C_p)_{Al2O3} + (\varphi\rho C_p)_{Cu} \quad (11)$$

whereas, $\varphi_{hnp} = \Phi_{Al2O3} + \varphi_{Cu}$, ρ_{hnf} is the effective density, ρ_{bhnf} is the coefficient of thermal expansion (16), and α_{hnf} is the thermal diffusivity of the hybrid nanofluid.

- Classical Maxwell's model [18]:

$$k_{hnf}/k_f = [k_{hnp} + 2k_f - 2\varphi_{hnp}(k_f - k_{hnp})] / [k_{hnp} + 2k_f + \varphi_{hnp}(k_f - k_{hnp})] \quad (12)$$

- Bruggeman's model [19]

$$k_{hnf} = (1/4) [(3\varphi_{hnp} - 1)k_{hnp} + (2 - 3\varphi_{hnp})k_f] + (k_f/4)\sqrt{\Delta} \quad (13)$$

$$\Delta = [(3\varphi_{hnp} - 1)^2 (k_{hnp} / k_f) + (2 - 3\varphi_{hnp})^2 + 2(2 + 9\varphi_{hnp} - 9\varphi_{hnp}^2) (k_{hnp} / k_f)] \quad (14)$$

whereas: $(k\varphi)_{hnp} = (k\varphi)_{Al2O3} + (k\varphi)_{Cu}$ (15)

It is important to note that since the volume fraction of copper is zero, all equations and relationships used for the Cu-Al₂O₃/water hybrid nanofluid are valid. In the equations above for the Cu-Al₂O₃/water hybrid nanofluid, the thermal conductivity values and the experimental values are provided by [17]. The solution is completed based on the experimental values of the thermal conductivity of the hybrid nanofluid, as the relationships provided by Maxwell and Bruggeman cannot accurately estimate the thermal conductivity values for the Cu-Al₂O₃/water hybrid nanofluid. To obtain the viscosity of the Cu-Al₂O₃/water hybrid nanofluid, the accuracy of the classical models used is examined as follows:

- Classical Models: Einstein's Model [20]

$$\mu_{hnf}/\mu_f = (1 + k_{\mu 1} * \varphi_{hnp}) \quad (16)$$

- Bruggeman model [21]

$$\mu_{hnf}/\mu_f = 1 / (1 - \varphi_{hnp})^{2.5} \quad (17)$$

- Batchelor model [22]

$$\mu_{hnf}/\mu_f = (1 + k_{\mu 1}.\varphi_{hnp} + k_{\mu 2}.\varphi_{hnp}) \quad (18)$$

$k_{\mu 1} = 2.5$ and $k_{\mu 2}$ is deviation from the maximum dilution limit of the suspension. As the volume fractions of Cu and Al₂O₃ nanoparticles increase, the viscosity increases. Using classical models underestimates the viscosity value. The boundary conditions in dimensionless form, can be written as by:

BC3: All the outer walls of the cavity

$$T=0, v=u=0 \quad (19a)$$

It is the specific heat capacity of the hybrid fluid.

$$\rho_{hnf} = \rho_f (1 - \varphi_{hnp}) + (\rho.\varphi)_{Al2O3} + (\rho.\varphi)_{Cu} \quad (9)$$

The following modified relationships were also obtained using the classical Maxwell [18] and Bruggeman [19] models to define the thermal conductivity of the hybrid nanofluid:

BC4: Oscillating cylinder (Temperature)

$$T=1 \quad (19b)$$

BC5: Oscillating cylinder (Motion)

$$u = 0; \quad v = \frac{dy}{dt} = 2A\pi f \cdot \cos(2\pi f\tau); \quad A = \frac{A^*}{L} \quad (19c)$$

The initial condition for the non-dimensional steady-state solution is considered for a cavity with a fixed cylinder at its center. In the non-dimensional thermal boundary condition, it is worth noting that the term in the sinusoidal function ($2\pi\tau$), which appears as a function $f = \omega L^2 / \alpha_f$ is the period of oscillation ($T_p = 1/f$), is equal to the inverse of the frequency. The local Nusselt number along the isothermal walls at the time dimension τ is calculated as follows:

$$Nu_{local} = - \left(\frac{k_{hnf}}{k_f} \right) \cdot \left(\frac{\partial T}{\partial n} \right)_{\tau} \quad (20)$$

n = direction normal to the walls By integrating the local Nusselt number Nu_{local} over time Nu_{avg} τ the average Nusselt number is obtained. The average temperature within the entire cavity can be calculated as follows:

$$Nu_{avg} = (1/W_0) \int_0^{W_0} Nu_{local} ds \quad (21)$$

$$T_{avg} = \left(\int_{\bar{v}} T_{local} d\bar{v} \right) / \left(\int_{\bar{v}} d\bar{v} \right) \quad (22)$$

Where W_0 = length of the hot cylinder. The fluid flow motion expressed as ψ is described as:

$$u = \frac{\partial \psi}{\partial y}; \quad v = - \frac{\partial \psi}{\partial x} \quad (23)$$

C. Mesh Validation:

An irregular triangular mesh was generated as shown in Fig (2).

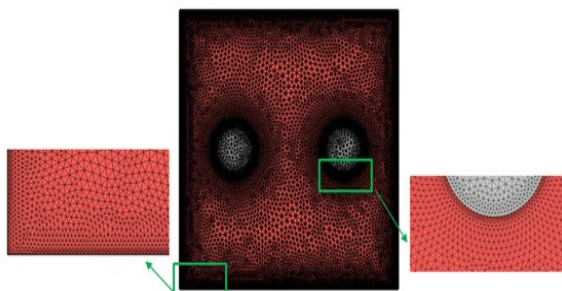


Figure 2: An irregular triangular network showing sharp gradients in temperature and speed.

To record steep temperature and velocity gradients, a suitable number of elements were concentrated near the perimeter of the cylinder and near its walls. Initially, a basic grid of 2406 elements were constructed, and the grid independence was systematically studied as the number of grids increased. To ensure the independence of the results from the number of grid elements, five different grid sizes were considered. Each grid size and its resulting Nusselt number are shown in Table 2.

The difference in the Nusselt number value for each grid size is also shown. It was observed that as the grid was further optimized from 3472 to 7928, the computational effort decreased by approximately 128.3%.

Table 2. Nusselt number for each mesh size

Grid independent test average Nusselt number on left cylinder surface at ($\phi_1=0.025$, $\phi_2=0.025$, $\phi=0.05$, $\tau=2$, $\Gamma=5$ 1/sec, $A=0.1$), two cylinder move to up and down.					
grid	domain elements	boundary elements	Time min	Nu_{ave}	Error %
G1	2406	164	60	4.4231	-
G2	3472	200	67	4.9962	11.4
G3	7928	404	77	5.1212	2.44
G4	23494	792	124	5.1260	0.09
G5	30020	892	154	5.1270	0.019

The results were compared using the COMSOL 2.6 software with published results by Debashis Dey and Sukanta K. Dash (23), which were simulated using Matlab b2016R software, to study natural convection heat transfer within a square cavity using ferro-hydraulic nanofluid (magnetic and non-magnetic). The comparison showed very good agreement at a concentration of $\phi=0.1\%$.

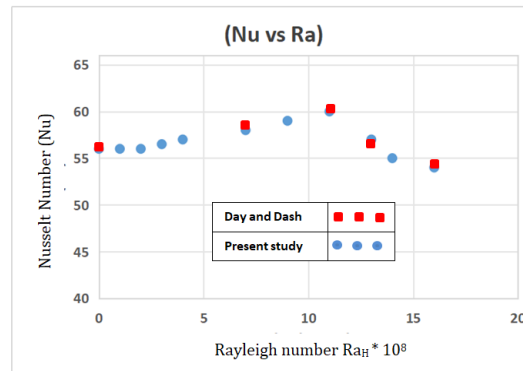


Figure 3: a) Flow lines, b) Isotherms

3. Results and Discussion

3.1. Stream Function

Fig. 4 shows the stream function of the fluid inside the cavity due to oscillatory motion of the horizontal cylinders at different values of Ra, amplitude, and frequencies.

The results show that, as a result of the vertical vibration of the heated cylinders inside the cavity, some vortices are presented. These vortices cover a large portion of the cavity. The vortices around the cylinder on the right side of the cavity are clockwise, while their direction in the cylinder on the left side of the cavity is counterclockwise. The greater the number of vortices, the more complex the flow becomes, and the lines begin to bend more as a result of turbulent flow. Increasing density of lines indicates increased velocity. The shifting of vortices from the middle to the edges indicates an increased effect of vibrations and natural convection within the cavity.

In addition, it is observed that with increasing the Rayleigh number from 10^3 and 10^5 at constant oscillation amplitude in Fig (4a) and constant frequency in Fig.(4b), the number of vortices generated around the heated cylinders increased.

This behaviour refers to a turbulent flow inside the cavity. Also, vortices are generated in the center of the top section of the cavity, and rotating in the opposite direction to the adjacent vortices. It is also observed that the flow velocity increases in the center and at the walls of the cavity for both variations in the frequencies and amplitudes of the cylinders. It is worth noting that, at Rayleigh 10^3 , new small vortices are generated between the cylinders and developed in the opposite direction to the large vortices. Size of these vortices increase with the increase in the oscillation amplitude, but they remain smaller than the large vortices. As the frequency increases, the generated small vortices become larger. This indicates that the flow has become more turbulent, which in turn, increases the heat transfer process. Also, the behavior around the two cylinders in all speed diagrams is asymmetrical.

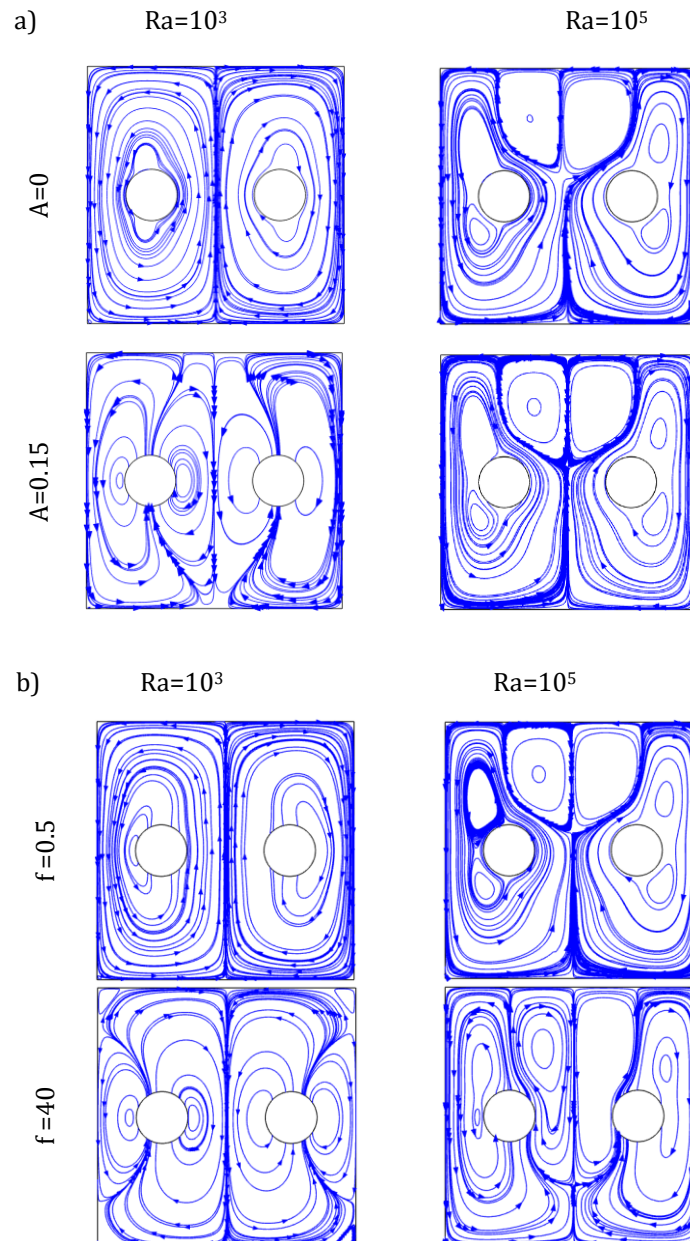


Figure 4: Velocity and direction chart at $Ra=10^3, 10^5, Di=2, \tau=2, \omega_{hpn}=0.5$: a) $f=2$, b) $A=0$

3.2 Isotherms and Heat Gradients

Fig. 5a and 5b show the isothermal curves of two oscillating cylinders at different values of the Rayleigh number with constant amplitude and frequency, respectively. In general, the isothermal curves are evenly distributed around the cylinders, becoming more concentrated at $Ra=10^3$. The isothermal curves are parallel to the heat source and the four cavity walls directly affected by it. As a result of the uniform heating of the cylinders and the continuous cooling of the cavity walls, the fluid behavior inside the cavity begins to change with increasing Ra .

The isothermal curves parallel to the walls tend to become more random and noticeably curved. The density of the isothermal lines increases around the

cylinders and near the upper cavity wall, and they are most concentrated above the cylinders. These lines taper off in the curve between the cylinders, giving a butterfly-like structure when $Ra=10^5$. The isothermal curves converge near the upper wall parallel to the cylinders with increasing Ra . This explains the transition from conduction to convection in the heat transfer mechanism. In other words, at lower values of Ra , the isotherms are evenly distributed around the cylinders in the center of the cavity. However, when Ra increased to 10^5 , the temperature gradient increased significantly toward the top of the cavity, i.e., above the two heated cylinders, and decreased between them and even below them. However, when the oscillation amplitude increased and the Rayleigh value was constant in Fig 5a, there was little change in the

temperature gradient within the cavity between the two cylinders. Furthermore, in Fig 5b, at $Ra = 10^3$, the temperature gradient began to increase toward the bottom of the cavity, with very little change at the top and sides of the cavity. As for Rayleigh 10^5 , it is observed that the thermal gradient starts from the upper surfaces of the heated cylinders towards the upper section of the cavity, with a slight change in the gradient behavior when the frequency value increases.

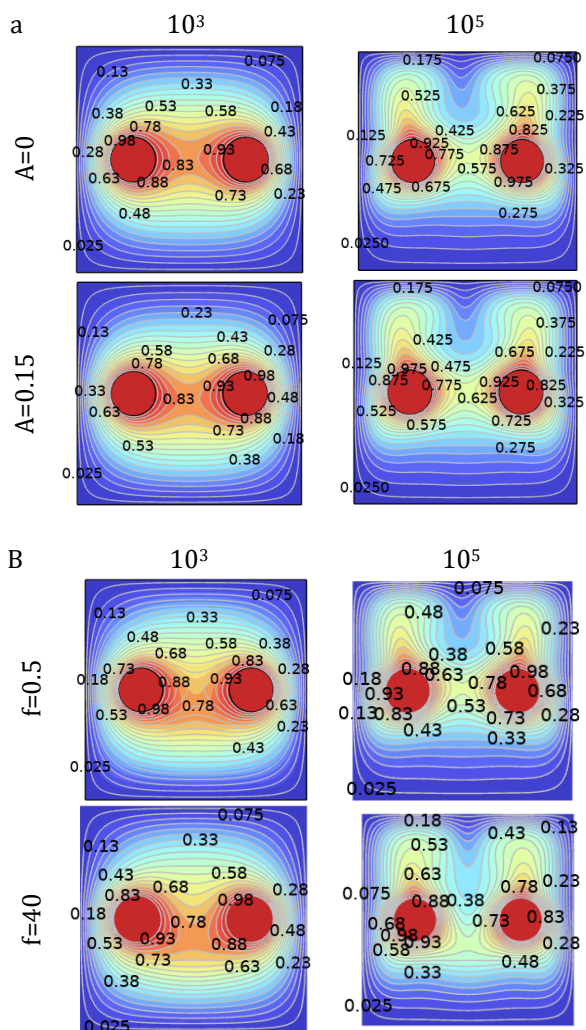


Figure 5: Isothermal of the two vibrating cylinders at Rayleigh numbers $10^3, 10^5$, $Di = 2$, $\tau = 2$, $\omega_{hpn} = 0.5$, a) $f=2$, b) $A=0.1$

3.3 Average Nusselt Value:

Table (3) and Table (4) show the average Nusselt values at different amplitudes and frequencies. In general, the interaction between the amplitude (A) and frequency (f), plays a critical role in affecting the average Nusselt values in noticeable ways. Larger amplitudes tend to generate greater turbulence in the flow. This turbulence improves convective heat transfer processes. Consequently, these values end up higher under those conditions. However, smaller

amplitudes usually lead to smoother laminar flow patterns.

Table 3. Average Nusselt number at $L = 0.62832$, $Di = 2$, $\tau = 2$, $\omega_{hpn} = 0.5$

Table (3)	Ra=10 ³		Ra=10 ⁵	
A	solid A	solid B	solid A	solid B
0	3.6083	3.6081	4.8495	4.8874
0.15	3.6411	3.6409	4.7502	4.7512

Table 4. Average number of offspring at, $L = 0.62832$, $Di = 2$, $\tau = 2$, $\omega_{hpn} = 0.5$

Table (4)	Ra=10 ³		Ra=10 ⁵	
f	solid A	solid B	solid A	solid B
0.5	3.6094	3.6092	4.8475	4.8522
40.000	3.6381	3.6378	4.9317	4.9321

Such patterns tend to lower the overall Nu. When the $Ra=10^3$, solids A and B display nearly identical Nu values in static conditions ($A=0$), around 3.608 for each. This similarity points to conduction as the primary mechanism at work. Introducing an amplitude of 0.15 causes a significant increase in Nu for both solids. Solid A hits 3.641, while solid B reaches 3.6409. These changes suggest that convection gets a slight boost from the oscillation. Shifting to a $Ra=10^5$ brings much higher Nu values as more intense natural convection effects. Solid A comes in at about 4.8495, and solid B at roughly 4.8874. However, applying an amplitude of 0.15 leads to a small drop in Nu across both solids. Solid A falls to 4.7502, with solid B at 4.7512. The evidence indicates that the oscillation interferes with the stronger convective streams in this regime.

In other words, greater frequency and amplitude typically support higher Nu through better mixing. However, higher values of oscillation starts to break up the flow structures in unhelpful ways. This can cause heat transfer gains to level off or even reverse. The trade-off between the frequency and amplitude of the oscillation is crucial for achieving peak efficiency in actual heat transfer setups.

4. Conclusions

Based on the results presented in the above section, some conclusion can be drawn as follows:

1. Increasing the oscillation amplitude from 0 to 0.15 and increasing the frequency from 0.5 to 40 did not significantly affect the thermal gradient compared to increasing the Rayleigh number from 10^3 to 10^5 . This indicates that motion of the cylinder vibration at high Rayleigh values enhances heat

transfer more than increasing the oscillation amplitude or frequency. Here, oscillatory motion demonstrates that it is a secondary dynamic factor that influences the fluid kinetic and temporal pattern. The primary determinant of the flow type within the cavity, whether conductive or convective, is the Raleigh number. At low Raleigh values, conductive heat transfer predominates, while at high Raleigh values, convection heat transfer becomes dominant.

2. At a Rayleigh value of 10^5 , the thermal gradient shifts toward the top of the cavity. This explains the strong convection generated by fluid movement, which draws heat from the bottom of the cavity to the top. Hot currents accumulate at the top of the cavity, generating thermal vortices, while the lower region becomes thermally semi-homogeneous.

3. The average Nusselt number shows a clear increase as the Rayleigh number increases from 10^3 to 10^5 . This is due to the dominance of convection heat transfer. Increasing the oscillation amplitude has a slight effect on the average Nusselt number at 10^3 , as heat transfer is nearly uniform. Convection becomes more turbulent with increasing Raleigh number, reducing the uniform mixing, leading to a decrease in the average Nusselt number with increasing Ra to 10^5 .

4. Increasing the frequency increases the average Nu, but to a lesser extent than the increase in Ra, which increases further when the number is increased to 10^5 , due to the high effect of Ra on convective heat transfer.

References

- [1] I. V. Miroshnichenko and M. A. Sheremet, "Turbulent natural convection heat transfer in rectangular enclosures using experimental and numerical approaches: a review," *Renew. Sustain. Energy Rev.*, vol. 82, pp. 40–59, 2018. DOI: 10.1016/j.rser.2017.09.005.
- [2] Roy, M, Das, D., and Basak, T., 2017. Studies on natural convection within enclosures of various (non-square) shapes–A review. *International Journal of Heat and Mass Transfer*, 106, pp.356-406.
- [3] Turkyilmazoglu, M., 2022. Exponential nonuniform wall heating of a square cavity and natural convection. *Chinese Journal of Physics*, 77, pp.2122-2135.D.
- [4] D. Das, M. Roy, and T. Basak, "Studies on natural convection within enclosures of various (non-square) shapes–A review," *Int. J. Heat Mass Transf.*, vol. 106, pp. 356–406, 2017. DOI: 10.1016/j.ijheatmasstransfer.2016.08.034.
- [5] Abdellahoum, C. and Mataoui, A., 2022. Effect of the Aspect Ratio on the heat transfer enhancement by the Al₂O₃-H₂O Nanofluid traversing a Heated Shallow Cavity. *WSEAS Transactions on Heat and Mass Transfer*, 17, pp.104-113.
- [6] S. Rostami, et al., "A review on the control parameters of natural convection in different shaped cavities with and without nanofluid," *Processes*, vol. 8, no. 9, pp. 1011, 2020. DOI: 10.3390/pr8091011.
- [7] Asmadi, M.S., Kasmani, R.M., Siri, Z., Saleh, H. and Ghani, N.C., 2023. Buoyancy-driven heat transfer performance, vorticity and fluid flow analysis of hybrid nanofluid within a U-shaped lid with heated corrugated wall. *Alexandria Engineering Journal*, 71, pp.21-38.
- [8] Ibrahim, M., Berrouk, A.S., Saeed, T. et al. Lattice Boltzmann-based numerical analysis of nanofluid natural convection in an inclined cavity subject to multiphysics fields. *Sci Rep* 12, 5514 (2022). <https://doi.org/10.1038/s41598-022-09320-8>
- [9] Chung, S. and Vafai, K., 2010. Vibration induced mixed convection in an open-ended obstructed cavity. *International journal of heat and mass transfer*, 53(13-14), pp.2703-2714.
- [10] Ayad S. Abedallah, Omar Rafae Alomar, Nabil J. Yasin, Numerical and experimental investigation on mixed convection heat transfer inside cavity heated from below with reciprocating moving upper surface, *International Communications in Heat and Mass Transfer*, Volume 159, Part C, 2024, 108242, ISSN 07351933, <https://doi.org/10.1016/j.icheatmasstransfer.2024.108242>.
- [11] D. Abdulsahib and K. Al-Farhany, "Experimental Investigation of Mixed Convection on a Rotating Circular Cylinder in a Cavity Filled With Nanofluid and Porous Media," *AL-QADISIYAH JOURNAL FOR ENGINEERING SCIENCES* 13 (2020)099-108
- [12] Al-Srayyih, B. M., Al-Manea, A., Saleh, K., Abed, A. M., Al-Amir, Q. R., Hamzah, H. K., ... Alahmer, A. (2023). Simulation investigation of the oscillatory motion of two elliptic obstacles located within a quarter-circle cavity filled with Cu-Al₂O₃/water hybrid nanofluid. *Numerical Heat Transfer, Part A: Applications*, 86(5), 1328–1352. <https://doi.org/10.1080/10407782.2023.227948>
- [13] -Mehryan, S.A.M., Izadpanahi, E., Ghalambaz, M. et al. Mixed convection flow caused by an oscillating cylinder in a square cavity filled with Cu–Al₂O₃/water hybrid nanofluid. *J Therm Anal Calorim* 137, 965–982 (2019). <https://doi.org/10.1007/s10973-019-08012-2>
- [14] Kefayati GR. Effect of a magnetic field on natural convection in an open cavity subjugated to water/alumina nanofluid using Lattice Boltzmann method. *Int Commun Heat Mass Transf.* 2013; 40:67–77.

- [15] Elshehabey HM, Hady F, Ahmed SE, Mohamed R. Numerical investigation for natural convection of a nanofluid in an inclined L-shaped cavity in the presence of an inclined magnetic field. *Int Commun Heat Mass Transf.* 2014; 57:228–38.
- [16] Nasrin R, Alim M. Free convective flow of nanofluid having two nanoparticles inside a complicated cavity. *Int J Heat Mass Transf.* 2013; 63:191–8.
- [17] Rashad A, Chamkha AJ, Ismael MA, Salah T. Magnetohydrodynamics natural convection in a triangular cavity filled with a Cu–Al₂O₃/water hybrid nanofluid with localized heating from below and internal heat generation. *J Heat Transf.* 2018; 140(7):072502
- [18] Maxwell JC. *A treatise on electricity and magnetism.* Oxford: Clarendon Press; 1881.
- [19] Hashim, Muhamad & Arifin, N. & Som, Ahmad & Ali, Nazihah & Ghani, Aniza & Ali, Safaa. (2023). Natural Convection in Trapezoidal Cavity containing Hybrid Nanofluid. *Journal of Advanced Research in Micro and Nano Engineering.* 13. 18-30. 10.37934/armne.13.1.1830.
- [20] Murshed S, Leong K, Yang C. Enhanced thermal conductivity of TiO₂—water based nanofluids. *Int J Therm Sci.* 2005;44(4):367–73.
- [21] Einstein A. *Investigations on the theory of the Brownian movement.* North Chelmsford: Courier Corporation; 1956.
- [22] Brinkman H. The viscosity of concentrated suspensions and solutions. *J Chem Phys.* 1952;20(4):571.
- [23] Debashis Dey, Sukanta K. Dash, An experimental investigation on the nanofluids in a cavity under natural convection with and without the rotary magnetic field, *Heliyon*, Volume 9, Issue 11, 2023, e22416, ISSN 2405-8440, <https://doi.org/10.1016/j.heliyon.2023.e22416>.